AEM
Journals.ASM.org

Differences in Physical and Biochemical Properties of *Thermus scotoductus* SA-01 Cultured with Dielectric or Convection Heating

Allison L. Cockrell,[a] Lisa A. Fitzgerald,[a] Kathleen D. Cusick,[a] Daniel E. Barlow,[a] Stanislav D. Tsoi,[a] Carissa M. Soto,[b] Jeffrey W. Baldwin,[c] Jason R. Dale,[d] Robert E. Morris,[a] Brenda J. Little,[d] Justin C. Biffinger[a]

Chemistry Division, U.S. Naval Research Laboratory, Washington, DC, USA[a]; Center for Bio/Molecular Science and Engineering, U.S. Naval Research Laboratory, Washington, DC, USA[b]; Acoustics Division, U.S. Naval Research Laboratory, Washington, DC, USA[c]; Geosciences Division, U.S. Naval Research Laboratory, Stennis Space Center, Mississippi, USA[d]

A thermophile, *Thermus scotoductus* SA-01, was cultured within a constant-temperature (65°C) microwave (MW) digester to determine if MW-specific effects influenced the growth and physiology of the organism. As a control, *T. scotoductus* cells were also cultured using convection heating at the same temperature as the MW studies. Cell growth was analyzed by optical density (OD) measurements, and cell morphologies were characterized using electron microscopy imaging (scanning electron microscopy [SEM] and transmission electron microscopy [TEM]), dynamic light scattering (DLS), and atomic force microscopy (AFM). Biophysical properties (i.e., turgor pressure) were also calculated with AFM, and biochemical compositions (i.e., proteins, nucleic acids, fatty acids) were analyzed by attenuated total reflectance-Fourier transform infrared (ATR-FTIR) spectroscopy. Gas chromatography-mass spectrometry (GC-MS) was used to analyze the fatty acid methyl esters extracted from cell membranes. Here we report successful cultivation of a thermophile with only dielectric heating. Under the MW conditions for growth, cell walls remained intact and there were no indications of membrane damage or cell leakage. Results from these studies also demonstrated that *T. scotoductus* cells grown with MW heating exhibited accelerated growth rates in addition to altered cell morphologies and biochemical compositions compared with oven-grown cells.

The term "extremophile" was first presented in 1974 by R. D. MacElroy to describe organisms that require extreme growth environments (or environments having conditions that humans cannot tolerate) (1). Since that time, thousands of extremophilic organisms have been identified in all three domains of the phylogenetic tree (*Bacteria*, *Archaea*, and *Eukarya*). These diverse organisms are further classified based on the environment in which they thrive. For example, thermophiles, like *Thermus aquaticus*, grow at high temperatures (>60°C) (2) while psychrophiles, e.g., *Cryomyces antarcticus*, prefer low temperatures (<15°C) (3). Members of the *Acidobacteria* phylum grow well in acidic environments (pH < 5) (4, 5) and are referred to as acidophiles. Barophiles or piezophiles such as *Shewanella benthica* require high pressures (>10 MPa) (6, 7), and halophiles like *Halomonas* spp. thrive in high-salt environments (up to 30%, wt/vol) (8). Some extremophiles thrive under multiple extreme conditions and are termed "polyextremophiles." For example, *Natranaerobius thermophilus* is an obligate anaerobic alkalithermophile that grows best at 55°C, 3.5 M Na^+, and pH 9.5 (9). The investigations of microbial communities that populate extreme environments such as hydrothermal vents and the Mariana trench have advanced our understanding of molecular and physiological responses underlying extremophile growth, survivability, and adaptation.

Over the years, the effects of low-frequency (3- to 300-GHz) radiation, or microwave (MW) radiation, on living microorganisms have been studied (see Fig. S1 in the supplemental material). However, there are limited data for specific nonthermal effects on microorganisms because (i) dielectric heating results in the residual heating of organisms and (ii) the only organisms studied have been mesophiles, or organisms that grow at moderate temperatures (20 to 45°C). By introducing multiple perturbations, the effects of low-frequency MW radiation on a biological system become unclear, and this has led to controversy in the literature. For example, in one study the mesophiles *Escherichia coli*, *Saccharomyces cerevisiae*, and *Salmonella enterica* were exposed to MW radiation or heated in a convection oven for various periods of time (up to 15 h) followed by growth and genetic analyses (10). Under both MW and oven conditions, the cells survived and showed similar growth rates, leading to the conclusion that MW-specific effects did not influence the growth or survivability of the cells (10). The results demonstrated that mesophiles can survive MW exposure, but the growth of these organisms during MW exposure was not addressed. A separate study found that MW heating, but not conventional heating, reversibly damaged the membranes in *Escherichia coli* (11). The authors concluded that there are specific nonthermal effects on bacteria that are induced by exposure to MW radiation (11). While the designs and results of these two studies were different, the authors agreed on one fundamental point, i.e., that it is difficult to distinguish between the effects of MWs and temperature on living microorganisms. However, if an organism thrives at elevated temperatures, then

Received 14 May 2015 **Accepted** 28 June 2015

Accepted manuscript posted online 6 July 2015

Citation Cockrell AL, Fitzgerald LA, Cusick KD, Barlow DE, Tsoi SD, Soto CM, Baldwin JW, Dale JR, Morris RE, Little BJ, Biffinger JC. 2015. Differences in physical and biochemical properties of *Thermus scotoductus* SA-01 cultured with dielectric or convection heating. Appl Environ Microbiol 81:6285–6293. doi:10.1128/AEM.01618-15.

Editor: R. M. Kelly

Address correspondence to Justin C. Biffinger, Justin.biffinger@nrl.navy.mil.

Supplemental material for this article may be found at http://dx.doi.org/10.1128/AEM.01618-15.

doi:10.1128/AEM.01618-15

potentially the thermal effects of dielectric heating from MW radiation can be separated.

During typical convection heating, the heat is transferred to a sample volume through the surface of the vessel to an internal material (i.e., cell culture). This heating method generally produces large thermal gradients and can result in uneven heating (i.e., the portion of the sample closest to the wall is the hottest, and the interior of the sample is the coolest) (12). Conversely, with MW heating the primary heating mechanism is through absorption of MW radiation by water and polar molecules to excite rotational energy levels, followed by nonradiative relaxation, which produces heating through friction (12). Some advantages of MW heating compared with convection heating include noncontact heating (no overheating of material surfaces), material selectivity (which affects dipole and charged molecules), and fast heating times (within minutes) (12). If the residual dielectric heating of an organism can be tolerated, then any resulting changes in physiology will primarily be a result of the MW radiation. To alleviate thermal effects and elucidate the impact of MW-specific effects on a microorganism, the thermophilic bacterium *Thermus scotoductus* SA-01 (with growth optimum at 65°C) was cultivated in an MW digester and a convection oven for 24 h. The growth, morphology, and biochemical compositions of these cells are reported to describe the physiological changes that occurred with MW heating. Since there are no prior physiological studies of thermophiles exposed to MW radiation, this study elucidates MW-specific effects on a thermophilic organism.

MATERIALS AND METHODS

Cell culture maintenance. *Thermus scotoductus* strain SA-01 was obtained from ATCC (ATCC 700910) and prepared according to the accompanying instructions. Briefly, the lyophilized stock was reconstituted using Castenholz-trypticase yeast extract (TYE) medium (ATCC medium 416). Stock cultures were aliquoted (200 μl) and stored at −80°C in 20% glycerol.

Cell growth conditions. For each experiment, 200 μl of frozen stock culture was grown in 10 ml of Castenholz-TYE medium at 65°C (Innova; New Brunswick Scientific) until it reached an optical density at 600 nm (OD_{600}) of 1.0 (24 h). From that culture, a 0.6-ml aliquot was transferred to a Teflon vessel (4.5 by 12 cm) containing 60 ml of Castenholz-TYE medium. Cells were grown in either a convection oven or an MW digester for 24 h. MW experiments were performed using a MARS 5 (CEM Corporation) system (2.45 GHz, 300-W power setting) with internal temperature control to maintain a temperature of 65°C throughout the experiment in all of the individual experiments simultaneously. The temperature probe was a standard microwave transparent probe (RTP-300) included with the MARS 5, which generates a feedback signal to the magnetron to regulate the power output. Detailed information of the MARS 5 system is provided in the supplemental information or online at the website of the CEM Corporation. The oven experiments were conducted using a convection incubator (New Brunswick Innova). The temperature was monitored with an optical probe placed in Castenholz-TYE medium (without cells) and was maintained at 65 ± 1°C for up to 30 h. A technical drawing of the MW digester system (MARS 5) used for these experiments is shown in Fig. S2 in the supplemental material.

Cell growth and viability. Oven- and MW-grown cell cultures were sampled (1 ml) every 2 h for up to 30 h. The OD_{600} of each sample was recorded, and then the sample was centrifuged at 12,000 × *g* for 3 min, the supernatant was removed from the cell pellet, and all samples were stored at −80°C. The supernatants and cell pellets were stored for ~1 month without a cryoprotectant and were used to determine extra- and intracellular protein and nucleic acid concentrations, respectively. To determine the cell viability after 24 h, an additional 1 ml of sample was collected and prepared using the Live/Dead BacLight bacterial viability assay kit according to the manufacturer's instructions (L-7007; Life Technologies) and visualized using a fluorescence microscope (Nikon). Student's *t* test was used for the 24-h time point to calculate the statistical significance of the OD_{600} data.

DLS analysis. Particle size was determined using a Brookhaven Instruments ZetaPALS dynamic light scattering (DLS) system, with BICW 32 software (Copyright 2005). In all measurements, 3 ml of cell culture was used in a 1-cm-diameter cuvette. For each size distribution, 10 measurements were taken at 25°C. Each size distribution measurement was performed in triplicate. An aliquot (3 ml) of the cell culture was collected after 24 h of growth in the MW or oven and was maintained in a water bath at 65°C prior to DLS analysis (within 30 min of collection). Due to the polydispersed nature of the samples, the lognormal size distribution output was selected as the data format. Lognormal distributions using the dust filter function of the software were exported directly from the instrument. Corresponding replicates were averaged and plotted.

SEM analysis. After 24 h, MW- and oven-grown cells were collected by centrifugation (3 min, 12,000 × *g*). The cell pellets were resuspended in 4% glutaraldehyde and stored at 4°C overnight. The next day, cells were washed 3 times with sterile irrigation water (BHL2F7114; Baxter Healthcare) and 2 μl of each sample was spotted onto a silicon wafer. The samples were dehydrated in an acetone (25%, 50%, 75%, 100%, 100%) series followed by dehydration in 100% ethanol (each ~2 to 3 min) and air dried as described previously (13). The samples were imaged with a Zeiss scanning electron microscope (SEM).

TEM analysis. For transmission electron microscopy (TEM) analysis, MW- or oven-grown cells (24 h) were collected and fixed as described above for SEM analysis. After fixation overnight in 4% glutaraldehyde, cells were washed 3 times with sterile irrigation water (BHL2F7114; Baxter Healthcare) and stored in 1× phosphate-buffered saline solution (0.1 M sodium phosphate, 0.15 M NaCl, pH 7.2). Cells were washed with 0.1 M sodium phosphate buffer (pH 7.2) and stained with 1% osmium tetroxide for 60 min. After rinsing again with sodium phosphate buffer, cells were embedded in agarose, cut into 1-mm^3 blocks, and dehydrated in an ethanol series (2 times in 50% ethanol for 10 min, 2 times in 70% ethanol for 10 min, 2 times in 95% ethanol for 10 min, and 3 times in 100% ethanol for 10 min). The dehydrated agarose blocks were infiltrated with 50% Spurr's low-viscosity resin (14) in 50% ethanol for 12 h, placed in fresh resin, and polymerized in an oven at 65°C for 48 h. Resin blocks were cut into thin sections (~70 nm) with an ultramicrotome (Leica Ultracut UCT), transferred to copper support grids, and imaged with a Zeiss EM109 transmission electron microscope operated at 80 kV.

Nucleic acid and protein determinations. Cells were grown as described either in a convection oven or under MW conditions for 24 h. For determinations of proteins and nucleic acids in supernatant samples, 1 ml of sample was collected from each culture vessel, the OD_{600} was recorded, and the sample was centrifuged (3 min, 12,000 × *g*). Supernatants were transferred to a separate tube, and the supernatants and pellets were stored at −80°C. Supernatant samples were thawed at room temperature (RT) and analyzed using a Nanodrop 2000 spectrometer (Fisher Scientific). Cell pellet samples were thawed and resuspended in ice-cold, freshly prepared lysis buffer (10 mM Tris-HCl [pH 8.0], 1 mM EDTA, 1% [wt/vol] Triton X-100, 1 mM phenylmethylsulfonyl fluoride, 0.01 mM pepstatin A, and 0.01 mM leupeptin). Cell suspensions were transferred to a 2-ml Eppendorf tube containing a cold, stainless steel bead (5 mm; Qiagen) and homogenized using two rounds of TissueLyser treatment (25 Hz, 2 min), with 1 min of cooling on ice between the treatments. Protein and nucleic acid concentrations in the cell lysates were analyzed using a Nanodrop 2000 spectrometer (Fisher Scientific). For each sample, the absorbance was collected to determine relative protein concentrations (A_{280}) and nucleic acid concentrations (A_{260}). Absolute nucleic acid concentrations (in micrograms per milliliter) and protein concentrations (in milligrams per milliliter) were calculated with the Nanodrop 2000 software. Statistical significance was calculated using Student's *t* test.

AFM analysis. *T. scotoductus* cells, grown in both convection and MW ovens for 24 h at 65°C in Castenholz-TYE medium, were used for atomic force microscopy (AFM) measurements. A cell pellet was collected by centrifuging the cultures for 5 min at 5,000 × *g*. The pellets were washed 3 times with sterile irrigation water and resuspended in sterile irrigation water (1:1, vol/vol). A 20-μl aliquot of each suspension was spread onto a glass slide and incubated at RT for 30 min. After this incubation, the slide was washed 3 times with sterile irrigation water and stored in sterile irrigation water until AFM measurements were collected (<1 h later). To promote bacterial adhesion, the glass slide was prepared 1 day before the experiment by covering the slide with 5 ml of poly-D-lysine. The slide was prepared with gentle shaking for 1 h at 37°C, followed by air drying for 24 h at RT. AFM measurements were carried out using Bruker Catalyst-Bio AFM mounted on an inverted optical microscope, and the samples were immersed in deionized water. A soft silicon nitride cantilever with a sharp tip (radius of curvature, ~20 nm) was used for all measurements. The stiffness of the cantilever ($k \approx 44$ pN/nm) was determined by measuring the thermal noise spectrum. All topography images were obtained using a PeakForce mode with a set point around 1 nN. The force curves were recorded from areas of the samples with adhered bacteria using the force-volume mode. The speed of the cantilever during approach/retract was set to 600 nm/s, and the transition from approach to retract was triggered when the repulsive force approached 1.6 nN. For each measured cell, two force curves with the greatest slope of the linear portion were selected and averaged to obtain the cell stiffness and uncertainty. Stiffness and topography measurements were used to calculate turgor pressure as described in supplemental materials and methods in the supplemental material. Briefly, the analysis presented in the supplemental information shows that in the first approximation the turgor pressure was proportional to $k_b R^{1/2}$, where $2R$ is the diameter of the cell (equal to the cell height in the topography image). Thus, using values of k_b and $2R$ determined from the stiffness and topography measurements, respectively, the turgor pressure was directly compared in individual bacterial cells.

ATR-FTIR measurements. After 24 h of growth in both the oven and MW, *T. scotoductus* cells were centrifuged at 5,000 × *g* for 5 min, washed 3 times with irrigation water, and placed on the attenuated total reflectance (ATR) element. When the bacteria were air dried, slight pressure was applied with the ATR anvil to ensure good contact to the ATR element. ATR-Fourier transform infrared (-FTIR) spectra were collected with a Thermo Scientific 6700 FTIR spectrometer, liquid nitrogen-cooled mercury cadmium telluride (MCT) detector, and Harrick SplitPea ATR microsampling accessory with a silicon ATR element. Spectra were collected at 4-cm^{-1} resolution and averaged for 256 scans. Absorbance spectra were referenced to the bare ATR element. These data were normalized to the peak at 1,541 cm^{-1}, as this band is attributed primarily to the amide II absorption of proteins and is generally unaffected by protein structural variations.

FAME extractions. After 24 h of heating, a 40-ml sample of each culture was centrifuged (5 min, 3,000 × *g*). The pellet was analyzed using published protocols for fatty acid methyl ester (FAME) (15). Briefly, the FAME extraction procedure involved harvesting the cells, saponification with rapid mixing and heat (3.8 M NaOH in 50% methanol), methylation at 80°C for 10 min (3.25 M HCl in 46% methanol), extraction using a 1:1 ratio of hexane and methyl-tert-butyl ether, and washing with 0.027 M NaOH. A single additional wash with 18 MΩ MilliQ water was performed to remove trace impurities. Samples were stored at −20°C before analysis.

Fatty acid analyses by GC-MS. Products in the FAME extracts were identified by gas chromatography-mass spectrometry (GC-MS). Data were acquired with an Agilent 7890A GC equipped with a standard multimode inlet and a 5975C mass selective detector. An Agilent autoinjector with a 10-μl syringe was used to introduce 1.0 μl of neat extract into the inlet, which was split at a 60:1 ratio. A DB-1ms (60 m by 0.25 mm by 0.50 μm film; Agilent) column was used with an oven temperature program that began at 40°C and was held for 1.5 min, ramped at 10°C/min to 290°C, and held for 10 min. The MS was scanned from 40 to 350 *m/z*, resulting in a scan rate of 5.19 Hz. A total of five replicate GC-MS analyses were obtained from each sample.

The MW-heated samples were compared with the oven-heated samples using a Fisher ratio (f-ratio) analysis (16) of the GC-MS data, which is capable of discerning very small differences between samples. The Fisher ratio is defined as the ratio of the variance between the two classes (MW, oven) and the variance between the replicates of a single sample. The f-ratio is a measure of how well each point in the total ion chromatogram describes the differences between the two classes. The f-ratio was then used to produce two feature selected data structures that represented the differences between the MW- and oven-heated samples. All compounds found in these feature selected data structures were identified by matching the mass spectra with archived library data through the NIST Mass Spectral Search Program for the NIST/EPA/NIH Mass Spectral Library (version 2.0g, 2011) (Scientific Instrument Services, Inc.).

RESULTS

Cell viability and growth during MW exposure. *T. scotoductus* cells were viable after 24 h of MW exposure (Fig. 1A to C). Cultures grown with convection heating also remained viable under the same conditions (i.e., medium, temperature, and time; see Fig. S3 in the supplemental material). OD_{600} analysis showed that cells grew to a significantly higher density and at a 10% higher rate in the MW than in the oven (Fig. 1D).

Cell morphologies during oven and MW growth. DLS data in Fig. 2 show that cells grown in the oven had a maximum size of 1,871 nm versus 4,690 nm for the MW-grown cells. A broader size distribution was obtained from the cells grown in the MW (1,831 to 12,111 nm) than from those grown in the oven (802 to 4,372 nm). The overall sizes of MW-grown cells were greater and the size population was more widely distributed than for the oven-grown cells.

SEM images showed that the oven-grown cells were ~2 μm long and well dispersed (Fig. 3A and B). MW-grown cultures, however, contained a greater distribution of elongated cells and contained aggregated cells and "chains" of cells (attached at the ends) that were not observed in oven-grown cultures (Fig. 3D and E). MW samples contained cells as short as 2 μm, with chains of cells reaching over 100 μm in length. Both TEM and AFM topography imaging showed that oven-grown cells were smaller than MW-grown cells (Fig. 3C and F and 4A, B, C, and D). Comparisons of cell morphology indicated that the MW-grown cells were longer and narrower than the oven-grown cells. Additional SEM, TEM, and AFM images and measurements are presented in Fig. S4 and S6 in the supplemental material. Imaging results confirmed the same general trends as the DLS data and demonstrated that 24 h of MW exposure led to aggregation and elongation of *T. scotoductus* cell cultures.

TEM images were also used to evaluate differences in intracellular structures between oven and MW cultures (Fig. 3C and F, respectively). While the cell sizes were different between *T. scotoductus* cells grown by the respective heating modes, the intracellular structures were very similar. These results indicated that MW treatment did not alter the intracellular membrane of *T. scotoductus* cells compared to conventional heating conditions. Additionally, the TEM images did not reveal any membrane damage. To determine whether the membrane integrity was compromised during MW exposure, culture supernatants were analyzed for changes in proteins and nucleic acids over time (see Fig. S5 in the supplemental material). The supernatant data indicated that the

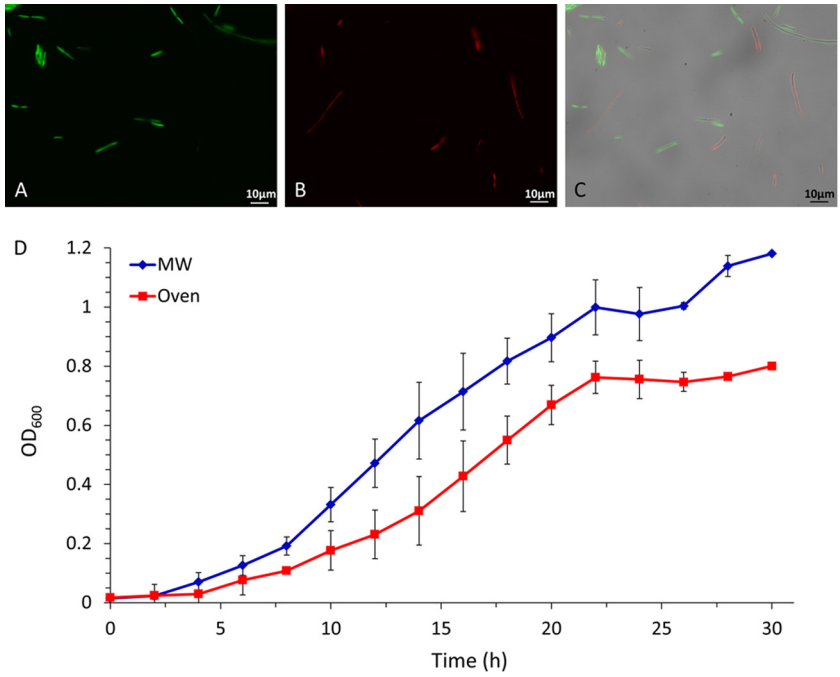

FIG 1 Viability and growth of *T. scotoductus* in an MW after 24 h. (A) Live cells; (B) dead cells; (C) overlay with phase contrast; (D) OD_{600} measurements of *T. scotoductus* growth under MW (blue) or oven (red) conditions. For MW data, $n = 7$, and for oven data, $n = 5$. Student's *t* test was performed using data collected at 24 h ($P < 0.05$).

concentrations of proteins and nucleic acids in the supernatants of oven-grown cells were comparable to those of MW-grown cells.

The comparison summarized for two MW- and three oven-grown cells in Fig. 4G and Table 1 suggested that despite the differences in their geometrical shape, MW growth did not appear to influence cell turgor pressures.

MW effects on cellular biochemical composition. Figure 5 shows overlaid ATR-FTIR spectra for cells grown in the MW or oven (24 h), normalized by the peak intensity at 1,541 cm^{-1}. The subtraction result for the normalized spectrum (results for oven subtracted from results for MW) is shown at the bottom of Fig. 5, and peak assignments are summarized in Table 2. The largest dif-

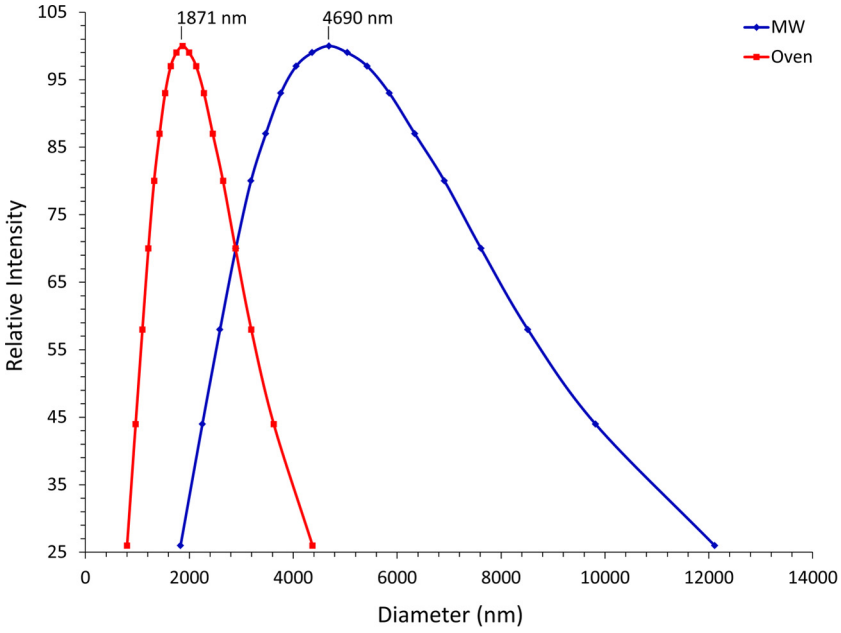

FIG 2 DLS analysis of *T. scotoductus* cultures grown in oven or MW. Cells were grown in the oven (red, $n = 2$) or MW (blue, $n = 3$) for 24 h, transferred to a 1-cm-path-length cuvette, and analyzed using a Brookhaven Instruments ZetaPALS DLS system at 25°C.

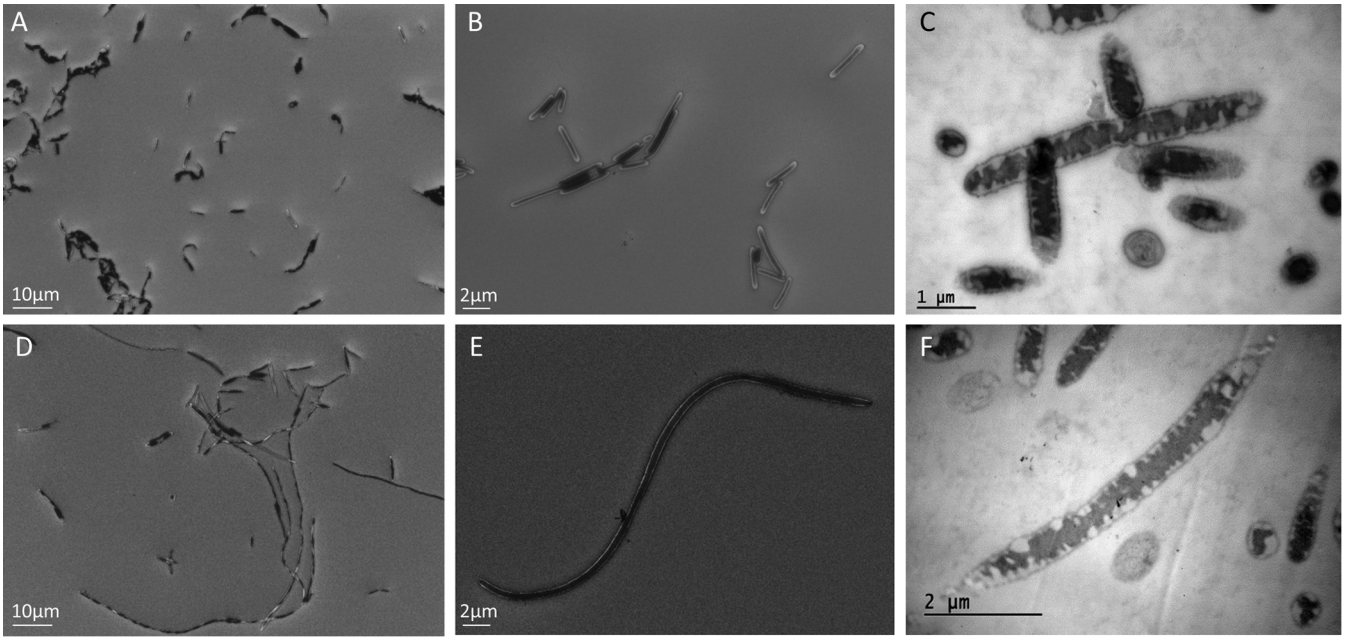

FIG 3 Images of *T. scotoductus* cells grown in the oven or MW. SEM images of cells grown for 24 h under oven (A and B) or MW (D and E) conditions. Images were obtained using a Zeiss scanning electron microscope with the following parameters: extrahigh tension (EHT), 10.00 kV; working distance (WD), 4.3 mm; magnification, ×1,000 (A and D) and ×3,500 (B and E). TEM images of cells grown under oven (C) or MW (F) conditions for 24 h. Images were obtained using a Zeiss EM109 transmission electron microscope operated at 80 kV and at a magnification of ×20,000. Images were collected from biological triplicate samples.

ferences in absorption intensities between the MW and oven spectra occurred at 1,083, 1,238, and 3,289 cm^{-1}. This can be observed in the overlaid spectra and in the difference spectrum (Fig. 5, green). Additional peaks were also observed in the difference spectrum at 1,604 cm^{-1} and 1,645 cm^{-1}, with shoulders extending to higher frequencies. The spectra in Fig. 5 show that intensity differences below ~1,750 cm^{-1} were due to additional absorptions in the MW-grown cells, while differences above ~2,700 cm^{-1} were due to additional absorptions in the oven-grown cells. The changes in FTIR peak intensities in Fig. 5 indicate differences in biochemical compositions of oven- and MW-grown cells. To determine if there were significant differences between concentrations of intracellular protein and nucleic acid concentrations, cell lysates were analyzed. These data show that cell lysates from oven-grown cultures contained slightly elevated protein and nucleic acid concentrations compared with MW-grown cultures (see Fig. S7 in the supplemental material).

Analysis of fatty acid (FA) compositions showed that oven-grown cells contained higher levels of total saturated FAs and fewer aromatic FAs than did MW-grown cells (Fig. 6). The largest differences in total heteroatom species were reflected in the concentrations of methyl esters, oxygen-bound, and isoalkane FAs (see Fig. S8 in the supplemental material). Oven-grown cells showed lower levels of methyl esters while oxygen-bound and isoalkane FAs were higher than in MW-grown cells. These analyses demonstrated that the biochemical compositions of cells were altered between MW and oven heating modes.

DISCUSSION

Here we report successful cultivation of a thermophile with only dielectric heating (Fig. 1). MW radiation (frequencies in the range of 0.1 to 10 cm; see Fig. S1 in the supplemental material) has many advantages compared to conventional (convection) heating. A dielectric material (i.e., aqueous medium) is directly heated by MW energy rather than by heat transfer through a material (i.e., vessel wall) (17). This process makes MW heating faster and more efficient than convection heating methods. Additionally, with MW heating, thermal gradients are minimized, creating a more evenly heated system than traditional convection heating.

Teflon, the material used in the vessels for both the MW and conventional oven experiments, has a low dielectric constant (2.1), which results in almost all of the applied MW energy being transferred to the aqueous medium and organisms rather than from the vessel to the medium. The penetration depth for water in an MW operating at 2.45 GHz, 300 W, and 65°C is ~4.7 cm and is a greater distance than the diameter of the vessels used for the culture experiments (4.5 cm). Moreover, the MARS 5 digester system is specifically designed to produce even heating among samples for extractions or organic synthesis reactions (18). Thus, this system was designed for parallel heating of several vessels to identical temperatures and exposure to the same level of microwave energy. The vessels containing culture medium were also preheated (24 h, 65°C) before inoculation to minimize thermal shock to the cells at the beginning of the experiment and minimize thermal gradients.

Cell growth and morphologies change based on heating mode. One of the most significant observations from the growth curves of *T. scotoductus* is that a 1.3-fold-higher OD was reached in the MW than in the oven (Fig. 1D) after 24 h of growth. The mechanisms behind this enhanced growth rate are unknown, but these results indicate that the MW treatment increased the cellular growth rate of *T. scotoductus*. Significant differences in cell morphology were also observed between *T. scotoductus* cells grown in an MW and those grown in an oven (Fig. 2 to 4). The elongated

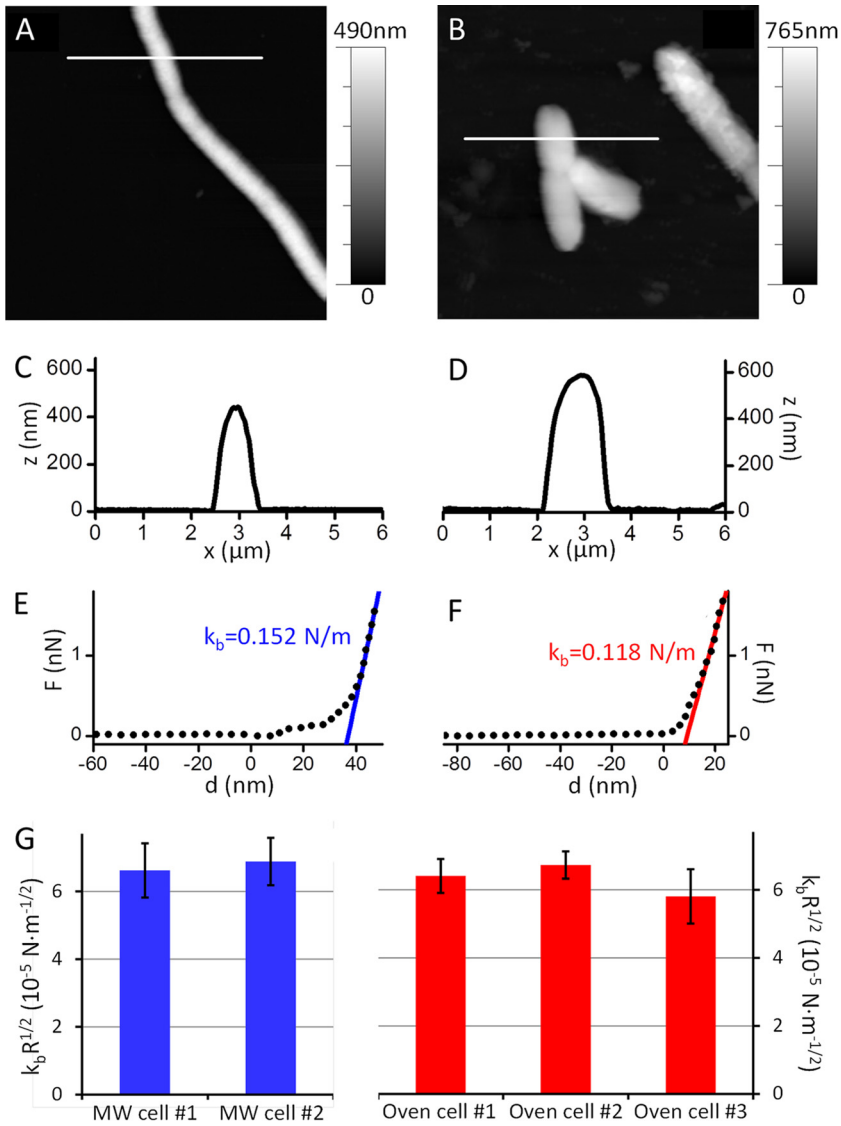

FIG 4 AFM analysis of MW- and oven-grown cells. AFM topography image of cells grown in an MW (A) or convection oven (B) for 24 h and then adhered to a glass substrate recorded in water. Image size, 10 μm by 10 μm. Data for cross-sections of the topography images in panels A and B taken along the white horizontal lines are shown in panels C and D, respectively. An $F(d)$ dependence recorded on the cells in images A and B is shown in panels E and F, respectively. (G) $k_bR^{1/2}$ values calculated for 2 MW-grown (blue) and 3 oven-grown (red) cells.

morphologies and "chains" of cells observed during MW growth have not been previously reported for *T. scotoductus* cultures. These morphologies have been observed when other *Thermus* species were grown under certain environmental conditions (19–22).

TABLE 1 Diameter and stiffness of MW- and oven-grown cells[a]

Cell growth condition and sample no.	$2R$ (10^{-7} m)	k_b (N · m^{-1})	p (10^{-5} N · m$^{-1/2}$)
MW sample 1	4.6 ± 0.1	0.138 ± 0.014	6.6 ± 0.8
MW sample 2	5.6 ± 0.1	0.130 ± 0.011	6.9 ± 0.7
Oven sample 1	6.0 ± 0.1	0.117 ± 0.007	6.4 ± 0.5
Oven sample 2	5.2 ± 0.1	0.132 ± 0.006	6.7 ± 0.4
Oven sample 3	6.0 ± 0.1	0.106 ± 0.012	5.8 ± 0.8

[a] The diameter and stiffness of individual cells were measured with AFM and calculated as $k_bR^{1/2}$, used as a measure of turgor pressure (p).

For example, *T. aquaticus* and *T. thermophilus* formed filaments when excess glycine (20 mM) was added to a culture medium and formed "chains of rods" when glycine was absent (19). The morphologies of *Thermus ruber* cells altered between rods and "long threads" as a result of the carbon source (21). More recently, the Δ*csaA* mutant of *T. thermophilus* HB-27 (70°C) displayed an elongated phenotype (the CsaA protein was predicted to play a role in cell wall synthesis) (22). In the work presented here, the only difference between culture conditions was the mode of heating (MW or convection). Therefore, the elongated morphologies observed with *T. scotoductus* cultures can be unambiguously attributed to MW-specific effects.

Cell integrity was not affected by MW exposure. The cellular membrane of a microorganism is the first level of protection against environmental perturbations (i.e., MW radiation). Three

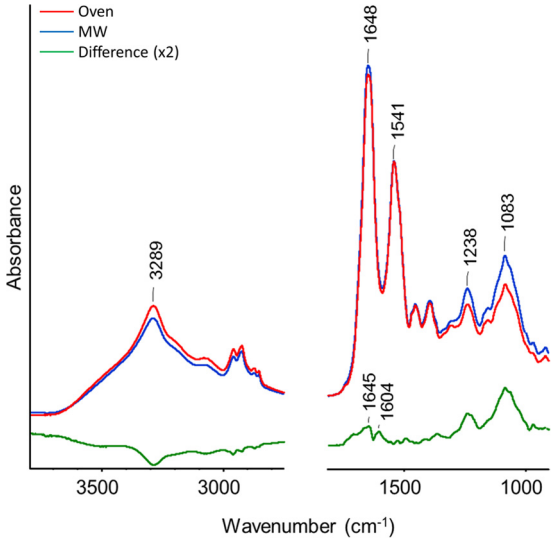

FIG 5 ATR-FTIR analysis of *T. scotoductus* cells grown in oven or MW environments. Normalized ATR-FTIR spectra of *T. scotoductus* grown in the MW (blue) or oven (red) for 24 h. The difference spectrum (MW − oven) is shown at the bottom and is multiplied by a factor of 2 (green). This analysis was performed for two biological replicate samples.

techniques were used to assess the impact of MW exposure on cell integrity: microscopy, supernatant analysis, and cell turgor pressure. *T. scotoductus* membranes appeared smooth and intact, and there was no apparent MW-induced membrane damage after 24 h of growth in either the MW or the oven (see Fig. S4A and B, respectively, in the supplemental material). These observations are in direct contrast to the observations published for mesophilic *E. coli* and *S. cerevisiae* cells exposed to MW radiation (11, 23). In *E. coli*, changes in cell morphology (described as a "dehydrated appearance") were reported after 540 s of MW exposure. The change was temporary, and after 10 min the cells recovered and were indistinguishable from control cells (11). *S. cerevisiae* cells also showed reversible cell membrane damage after low doses of MW radiation (100 W, 90 s) and irreversible cell membrane damage after higher doses (220 W, 90 s) (23). However, with *T. scotoductus* no membrane damage was detected by SEM or TEM after 24 h (or 86,400 s) of MW heating (300 W) (Fig. 3; see also Fig. S4 in the supplemental material). The thermophilic nature of *T. scotoductus* allows for this organism to survive at elevated temperatures, and the microscopy results confirmed that specific MW effects did not lead to visible membrane damage in this microorganism.

Supernatant concentrations of proteins and nucleic acids also showed little to no variation between samples over the 24-h sampling period (see Fig. S5 in the supplemental material). In the previously mentioned *E. coli* and *S. cerevisiae* studies, pores were formed in the membranes during MW exposure and were repaired when cells were allowed to recover (11, 23). In the case of reversible pore formation, the supernatant concentrations of intracellular components (i.e., proteins and nucleic acids) increased over time (11, 23). With *T. scotoductus*, the supernatant concentrations of proteins and nucleic acids were the same between MW- and oven-grown cultures, indicating that reversible pore formation did not occur in these studies. The similar concentrations of nucleic acids in the supernatants indicated that there was not an increase in cell lysis from one heating mode to another. These results confirmed the conclusions made from the SEM and TEM images and indicated that specific MW effects did not induce membrane damage on *T. scotoductus* cells.

The last measure of membrane integrity was obtained by calculating the intracellular turgor pressures in MW- and oven-grown cells with AFM. Cell turgor pressure is crucial for maintaining proper cell structure and functionality (24, 25), and in this type of experiment the AFM tip pushes on a cell surface and the force (F) required to compress (indent) the cell by a distance (d) is measured. Figure 4E and F present typical $F(d)$ dependencies recorded on the MW- and oven-grown cells shown in Fig. 4A and B, respectively. Declines in turgor pressures after treatment can indicate pore formation or leakage of intracellular components. For example, in previous AFM studies the mesophilic bacteria *Bacillus subtilis*, *Planococcus maritimus*, and *Staphylococcus aureus* displayed lower turgor pressures after MW exposure than prior to MW exposure (26). Conversely, in the AFM studies of *T. scotoductus* the turgor pressures were similar for cells grown under MW and oven conditions. These data demonstrate that MW-specific effects did not affect cellular turgor pressures in *T. scotoductus* (Fig. 4) and that specific MW effects did not promote membrane damage in *T. scotoductus* cells.

Differences in MW- and oven-treated cell biochemical compositions. MW-induced changes in cellular biochemical compositions (i.e., proteins, nucleic acids, fatty acids) have also been reported (27, 28), and differences in the vibrational (IR) spectra of bacteria can be correlated with physiological differences (29–31). Thus, the changes in FTIR peak intensities shown in Fig. 5 were used to observe potential differences in proteins, lipids, polysaccharides, or nucleic acids from oven- and MW-grown *T. scotoductus* (29–31). The absorption bands in the MW and oven spectra all showed similar positions, but with some differences in intensities. For example, the intensity differences from 2,500 to 3,500 cm^{-1} (Fig. 5) indicated that MW samples contained lower concentrations of lipids and carbohydrates and displayed different protein structural contents from those of oven samples. The enhanced signal intensities from 1,000 to 1,700 cm^{-1} were attributed to increased concentrations of polysaccharides, phospholipids, and nucleic acids in MW versus oven samples (29–31).

These differences in FTIR intensity indicated that specific MW effects influenced the biochemical composition of *T. scotoductus*

TABLE 2 ATR-FTIR peak assignments[a]

Frequency (cm^{-1})	Vibration	Related material(s)
3,289	Amide A [ν(N—H)]; ν(OH)	Side chains, water, carbohydrate
2,959	ν_a (CH3)	Lipid, side chains
2,925	ν_a (CH2)	Lipid, side chains
2,874	ν_s (CH3)	Lipid, side chains
2,854	ν_s (CH2)	Lipid, side chains
1,648	Amide I [ν(C=O)]	Protein
1,541	Amide II, protein; ν (COO^-)	Protein, side chains
1,238	$\nu_a(PO2^-)$; ν(C—O); amide III	Protein, phospholipids, polysaccharides, nucleic acids
1,083	$\nu_s(PO2^-)$; ν(C—O)	Phospholipids, polysaccharides, nucleic acids

[a] Assignments correspond to the spectra shown in Fig. 5. For more information, see references 40 and 41.

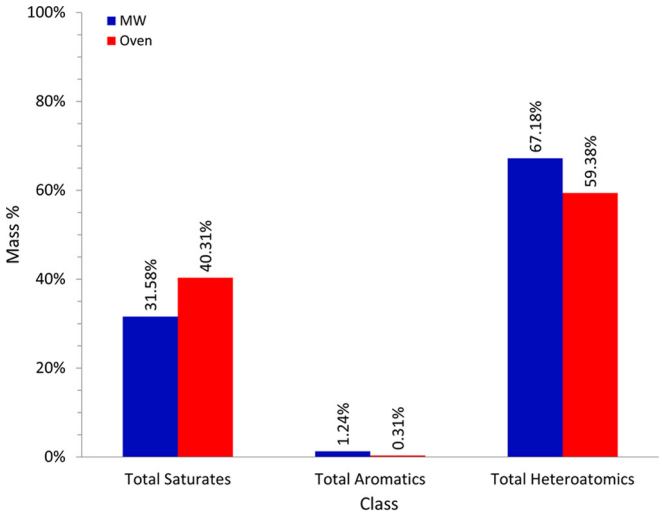

FIG 6 FA analysis of MW and oven samples. Mass percentages of FAMEs observed in samples prepared from cells grown under MW (blue) or oven (red) conditions for 24 h. These data represent results from one of three biological replicate samples.

cells (29–31). MW radiation has been hypothesized to denature proteins by disrupting hydrogen bonding networks between amino acid side chains and thus protein secondary structures (32). This effect arises from the physical perturbations that MW frequencies induce on polar molecules (i.e., amino acid side chains) (33). The FTIR signals related to protein content, lipids, and carbohydrates (>2,500 cm^{-1}) showed lower intensities in MW- than in oven-grown cells, indicating that MW exposure led to a decline in these species.

The FTIR peak intensities at 1,238 and 1,083 cm^{-1}, which were attributed to changes in polysaccharides, phospholipids, and nucleic acids, suggested that MW-grown cells contained more of these species than did oven-grown cells (Fig. 5). However, the quantitative analysis of nucleic acid concentrations in cell lysates showed that MW-grown cells contained lower nucleic acid concentrations than did oven-grown cells (see Fig. S7 in the supplemental material). Therefore, the relatively higher intensities at 1,238 and 1,083 cm^{-1} should be more likely attributed to elevated levels of polysaccharides and/or phospholipids in MW-grown cells than to increased nucleic acid concentrations. Studies with mesophiles have reported a decline in nucleic acid concentrations after MW exposure (27), and the data reported here agree with that observation. These data also indicate that MW-specific effects promoted polysaccharide and/or phospholipid concentrations and negatively influenced nucleic acid concentrations.

Structural and chemical changes due to dielectric heating could also be manifested in the cellular fatty acid content. FAME analysis of the fatty acids extracted from cells after 24 h (Fig. 6) showed that there were notable differences between the FA compositions of cells grown in the oven and those grown in an MW, based on compound class. Our FAME results are consistent with changes in FA composition resulting from exposure of *Salmonella* Typhimurium to MW radiation (28). Bacterial adaptation to stress has been associated with an increase in the concentration of unsaturated FAs (28, 34). In *S.* Typhimurium, short-duration MW exposure led to lower levels of saturated FAs (28). Decreases in saturated FA content were also observed in the present studies, as the mass percentage of total saturated FAs in *T. scotoductus* were 8.8% lower during MW growth than during oven growth (Fig. 6). These results could suggest that the unsaturated FA content reflected a MW-induced stress response in *T. scotoductus* cells.

Data describing the physiological response of a thermophile exposed to MW radiation demonstrated several significant differences from literature precedents using mesophilic bacteria and yeast. By conducting experiments with two variables (thermal and specific MW effects), controversy arises over how to differentiate between specific MW effects and thermal effects (35). The advantage of using a thermophile, e.g., *T. scotoductus*, for MW experiments is that the elevated temperatures (>60°C) resulting from MW heating are suitable for culturing (36) and result in viable cells and enhanced growth. Therefore, in the experiments presented here, the thermal effects of convection and MW heating modes were eliminated and the differences between these heating modes on a culture could be observed. Using a thermophile for MW experiments is a logical first step to understanding the effects of microwave energy on a living microorganism (37–39).

Conclusions. Our data demonstrated that the thermophilic bacterium *T. scotoductus* can be cultured during prolonged MW exposure (2.45 GHz, 24 h). Growth curves revealed that *T. scotoductus* grew at a slightly higher rate and reached a higher OD under MW than under oven conditions. SEM and TEM imaging analysis showed that the morphologies of MW-grown cells were dramatically different from those of oven-grown cells. Specifically, MW-grown cells were elongated and formed chains of cells which were >100 μm in length, while oven-grown cells were more homogenous and cell lengths ranged from ~1.5 to 4 μm. Biochemical analyses showed that the MW growth conditions also led to decreased protein and nucleic acid concentrations and promoted unsaturated FA production. Biophysical studies showed that MW growth did not influence the cellular turgor pressures. Nucleic acid and protein leakage assays indicated that the cell membranes were intact after 24 h of growth in both MW and oven.

The cultivation method presented here provides a unique opportunity to investigate the influences of specific MW effects on living organisms, and future analyses could be conducted to probe specific physiological changes (i.e., antibiotic resistance, biofilm formation, pigmentation level) and to define the timing and effects of additional environmental perturbations (i.e., pH, medium composition) using microwave energy. Culturing *Thermus* using microwave energy also makes it possible to determine if specific nonthermal MW effects induce mutagenesis or systematic changes in transcriptional profiles using a living organism.

Using extremophiles to study the effects of MW radiation allows for thermal MW effects on the biological system to be essentially negated and specific MW effects to be potentially evaluated. Collectively, these results support the hypothesis that MW heating affects the physiology of biological systems. Developing a greater understanding of how organisms survive and thrive in extreme environments, such as being heated with microwave radiation, could significantly alter culture methods for biotechnologically relevant microorganisms.

ACKNOWLEDGMENTS

This work was funded by ONR/NRL Blk 6.1 Nanoscience Institute funding. We thank the National Research Council for A.L.C.'s and K.D.C.'s postdoctoral research associateships.

We acknowledge Christopher Spillman for use of the fluorescence

microscope, and we thank Kenneth J. Curry and Jessica R. Douglas of the University of Southern Mississippi, School of Polymers and High Performance Materials, for assistance with transmission electron microscopy.

REFERENCES

1. **Macelroy RD.** 1974. Some comments on evolution of extremophiles. Biosystems **6:**74–75. http://dx.doi.org/10.1016/0303-2647(74)90026-4.
2. **Canganella F, Wiegel J.** 2014. Anaerobic thermophiles. Life (Basel) **4:**77–104 http://dx.doi.org/10.3390/life4010077.
3. **Sterflinger K, Lopandic K, Pandey RV, Blasi B, Kriegner A.** 2014. Nothing special in the specialist? Draft genome sequence of *Cryomyces antarcticus*, the most extremophilic fungus from Antarctica. PLoS One **9:**e109908. http://dx.doi.org/10.1371/journal.pone.0109908.
4. **Dopson M, Ossandon FJ, Lovgren L, Holmes DS.** 2014. Metal resistance or tolerance? Acidophiles confront high metal loads via both abiotic and biotic mechanisms. Front Microbiol **5:**157. http://dx.doi.org/10.3389/fmicb.2014.00157.
5. **Ward NL, Challacombe JF, Janssen PH, Henrissat B, Coutinho PM, Wu M, Xie G, Haft DH, Sait M, Badger J, Barabote RD, Bradley B, Brettin TS, Brinkac LM, Bruce D, Creasy T, Daugherty SC, Davidsen TM, Deboy RT, Detter JC, Dodson RJ, Durkin AS, Ganapathy A, Gwinn-Giglio M, Han CS, Khouri H, Kiss H, Kothari SP, Madupu R, Nelson KE, Nelson WC, Paulsen I, Penn K, Ren QH, Rosovitz MJ, Selengut JD, Shrivastava S, Sullivan SA, Tapia R, Thompson LS, Watkins KL, Yang Q, Yu CH, Zafar N, Zhou LW, Kuske CR.** 2009. Three genomes from the phylum *Acidobacteria* provide insight into the lifestyles of these microorganisms in soils. Appl Environ Microbiol **75:**2046–2056. http://dx.doi.org/10.1128/AEM.02294-08.
6. **Picard A, Daniel I.** 2013. Pressure as an environmental parameter for microbial life—a review. Biophys Chem **183:**30–41. http://dx.doi.org/10.1016/j.bpc.2013.06.019.
7. **Kato C, Bartlett DH.** 1997. The molecular biology of barophilic bacteria. Extremophiles **1:**111–116. http://dx.doi.org/10.1007/s007920050023.
8. **Kim KK, Lee JS, Stevens DA.** 2013. Microbiology and epidemiology of *Halomonas* species. Future Microbiol **8:**1559–1573. http://dx.doi.org/10.2217/fmb.13.108.
9. **Zhao BS, Mesbah NM, Dalin E, Goodwin L, Nolan M, Pitluck S, Chertkov O, Brettin TS, Han J, Larimer FW, Land ML, Hauser L, Kyrpides N, Wiegel J.** 2011. Complete genome sequence of the anaerobic, halophilic alkalithermophile *Natranaerobius thermophilus* JW/NM-WN-LF. J Bacteriol **193:**4023–4024. http://dx.doi.org/10.1128/JB.05157-11.
10. **Dutta SK.** 1980. Genetic and cellular effects of microwave radiations. U.S. Environmental Protection Agency, Research Triangle Park, NC.
11. **Shamis Y, Taube A, Mitik-Dineva N, Croft R, Crawford RJ, Ivanova EP.** 2011. Specific electromagnetic effects of microwave radiation on *Escherichia coli*. Appl Environ Microbiol **77:**3017–3022. http://dx.doi.org/10.1128/AEM.01899-10.
12. **Gude PP, Martinez-Guerra VGE, Deng S, Nirmalakhandan N.** 2013. Microwave energy potential for biodiesel production. Sustainable Chem Processes **1:**1–31. http://dx.doi.org/10.1186/2043-7129-1-1.
13. **Ray R, Lizewski S, Fitzgerald LA, Little B, Ringeisen BR.** 2010. Methods for imaging *Shewanella oneidensis* MR-1 nanofilaments. J Microbiol Methods **82:**187–191. http://dx.doi.org/10.1016/j.mimet.2010.05.011.
14. **Spurr AR.** 1969. A low-viscosity epoxy resin embedding medium for electron microscopy. J Ultrastruct Res **26:**31–43. http://dx.doi.org/10.1016/S0022-5320(69)90033-1.
15. **Eder K.** 1995. Gas-chromatographic analysis of fatty-acid methylesters. J Chromatogr B **671:**113–131. http://dx.doi.org/10.1016/0378-4347(95)00142-6.
16. **Johnson KJ, Rose-Pehrsson SL, Morris RE.** 2004. Monitoring diesel fuel degradation by gas chromatography-mass spectroscopy and chemometric analysis. Energy Fuels **18:**844–850. http://dx.doi.org/10.1021/ef030161z.
17. **Dale ECS, Compton RG, Marken F.** 2012. Microwaves and electrochemistry, p 525–539. *In* Loupy A, de la Hoz A (ed), Microwaves in organic synthesis, 3rd ed, vol 1. John Wiley & Sons, New York, NY.
18. **CEM Corporation.** 2001. MARS 5: microwave accelerated reaction system user manual. CEM Corporation, Matthews, NC.
19. **Janssen PH, Parker LE, Morgan HW.** 1991. Filament formation in *Thermus* species in the presence of some D-amino acids or glycine. Antonie Van Leeuwenhoek **59:**147–154.
20. **Brock TD, Freeze H.** 1969. *Thermus aquaticus* gen. n. and sp. n., a nonsporulating extreme thermophile. J Bacteriol **98:**289–297.
21. **Loginova LG, Khraptsova GI.** 1977. Effect of carbon source on the development of *Thermus ruber* at different temperatures. Mikrobiologiya **46:**38–40.
22. **Acosta F, de Pedro MA, Berenguer J.** 2012. Homogeneous incorporation of secondary cell wall polysaccharides to the cell wall of *Thermus thermophilus* HB27. Extremophiles **16:**485–495. http://dx.doi.org/10.1007/s00792-012-0448-x.
23. **Zeng SW, Huang QL, Zhao SM.** 2014. Effects of microwave irradiation dose and time on yeast ZSM-001 growth and cell membrane permeability. Food Control **46:**360–367. http://dx.doi.org/10.1016/j.foodcont.2014.05.053.
24. **Margolin W.** 2009. Sculpting the bacterial cell. Curr Biol **19:**R812–R822. http://dx.doi.org/10.1016/j.cub.2009.06.033.
25. **Arnoldi M, Fritz M, Bauerlein E, Radmacher M, Sackmann E, Boulbitch A.** 2000. Bacterial turgor pressure can be measured by atomic force microscopy. Phys Rev E **62:**1034–1044. http://dx.doi.org/10.1103/PhysRevE.62.1034.
26. **Pogodin S, Hasan J, Baulin VA, Webb HK, Truong VK, Nguyen THP, Boshkovikj V, Fluke CJ, Watson GS, Watson JA, Crawford RJ, Ivanova EP.** 2013. Biophysical model of bacterial cell interactions with nanopatterned cicada wing surfaces. Biophys J **104:**835–840. http://dx.doi.org/10.1016/j.bpj.2012.12.046.
27. **Das RH, Ahirwar R, Kumar S, Nahar P.** 2015. Microwave-mediated enzymatic modifications of DNA. Anal Biochem **471:**26–28. http://dx.doi.org/10.1016/j.ab.2014.11.003.
28. **Nasri K, Daghfous D, Landoulsi A.** 2013. Effects of microwave (2.45 GHz) irradiation on some biological characters of *Salmonella typhimurium*. C R Biol **336:**194–202. http://dx.doi.org/10.1016/j.crvi.2013.04.003.
29. **Beekes M, Lasch P, Naumann D.** 2007. Analytical applications of Fourier transform-infrared (FT-IR) spectroscopy in microbiology and prion research. Vet Microbiol **123:**305–319. http://dx.doi.org/10.1016/j.vetmic.2007.04.010.
30. **Clemens G, Hands JR, Dorling KM, Baker MJ.** 2014. Vibrational spectroscopic methods for cytology and cellular research. Analyst **139:**4411–4444. http://dx.doi.org/10.1039/C4AN00636D.
31. **Maquelin K, Kirschner C, Choo-Smith LP, van den Braak N, Endtz HP, Naumann D, Puppels GJ.** 2002. Identification of medically relevant microorganisms by vibrational spectroscopy. J Microbiol Methods **51:**255–271. http://dx.doi.org/10.1016/S0167-7012(02)00127-6.
32. **Lill JR, Ingle ES, Liu PS, Pham V, Sandoval WN.** 2007. Microwave-assisted proteomics. Mass Spectrom Rev **26:**657–671. http://dx.doi.org/10.1002/mas.20140.
33. **Challis LJ.** 2005. Mechanisms for interaction between RF fields and biological tissue. Bioelectromagnetics **2005**(Suppl 7)**:**S98–S106.
34. **Sampathkumar B, Khachatourians GG, Korber DR.** 2004. Treatment of *Salmonella enterica* serovar Enteritidis with a sublethal concentration of trisodium phosphate or alkaline pH induces thermotolerance. Appl Environ Microbiol **70:**4613–4620. http://dx.doi.org/10.1128/AEM.70.8.4613-4620.2004.
35. **Shamis Y, Croft R, Taube A, Crawford RJ, Ivanova EP.** 2012. Review of the specific effects of microwave radiation on bacterial cells. Appl Microbiol Biotechnol **96:**319–325. http://dx.doi.org/10.1007/s00253-012-4339-y.
36. **Balkwill DL, Kieft TL, Tsukuda T, Kostandarithes HM, Onstott TC, Macnaughton S, Bownas J, Fredrickson JK.** 2004. Identification of iron-reducing *Thermus* strains as *Thermus scotoductus*. Extremophiles **8:**37–44. http://dx.doi.org/10.1007/s00792-003-0357-0.
37. **Oliveira EA, Nogueira NGP, Innocentini MDM, Pisani R.** 2010. Microwave inactivation of *Bacillus atrophaeus* spores in healthcare waste. Waste Manage **30:**2327–2335. http://dx.doi.org/10.1016/j.wasman.2010.05.002.
38. **Yu Y, Lo IW, Chan WWI, Liao PH, Lo KV.** 2010. Nutrient release from extracted activated sludge cells using the microwave enhanced advanced oxidation process. J Environ Sci Health A Tox Hazard Subst Environ Eng **45:**1071–1075. http://dx.doi.org/10.1080/10934529.2010.486332.
39. **Kim SY, Jo EK, Kim HJ, Bai K, Park JK.** 2008. The effects of high-power microwaves on the ultrastructure of *Bacillus subtilis*. Lett Appl Microbiol **47:**35–40. http://dx.doi.org/10.1111/j.1472-765X.2008.02384.x.
40. **Barth A.** 2007. Infrared spectroscopy of proteins. Biochim Biophys Acta **1767:**1073–1101. http://dx.doi.org/10.1016/j.bbabio.2007.06.004.
41. **Quiles F, Humbert F, Delille A.** 2010. Analysis of changes in attenuated total reflection FTIR fingerprints of *Pseudomonas fluorescens* from planktonic state to nascent biofilm state. Spectrochim Acta A Mol Biomol Spectrosc **75:**610–616. http://dx.doi.org/10.1016/j.saa.2009.11.026.